COMPUTATIONAL STUDIES OF THREE-DIMENSIONAL OCEAN SOUND FIELDS IN AREAS OF COMPLEX SEAFLOOR TOPOGRAPHY AND ACTIVE OCEAN DYNAMICS

TIMOTHY F. DUDA [1]
YING-TSONG LIN [1]
WEIFENG GORDON ZHANG [1]
BRUCE D. CORNUELLE [2]
PIERRE F. J. LERMUSIAUX [3]

[1] *Woods Hole Oceanographic Institution*
WHOI AOPE Dept. MS 11
Woods Hole, Massachusetts 02543
United States of America
email: tduda@whoi.edu, ytlin@whoi.edu, wzhang@whoi.edu

[2] *Scripps Institution of Oceanography*
University of California, San Diego
La Jolla, California 92093-0225
United States of America
email: bdc@ucsd.edu

[3] *Massachusetts Institute of Technology*
77 Massachusetts Avenue
Cambridge, Massachusetts 02139-430
United States of America
email: pierrel@mit.edu

Time-evolving three-dimensional (four-dimensional) numerical modeling of sound is performed for ocean environmental conditions calculated using regional ocean flow models. The flow models solve the appropriate nonlinear equations in bands of resolved scales and frequencies. Subgrid scale processes are parameterized, as are boundary processes. The ocean fields are interpolated onto acoustic model grids that are two orders of magnitude tighter than the flow model grids. The computations provide reliable estimates of the acoustic effects of the resolved ocean processes such as geostrophic currents, mixed-layer changes, and internal tides, but they do not include the acoustic implications of unresolved structures such as nonlinear internal waves, sharp boundary layers, and small-scale intrusions. Examples of complicated sound fields from resolved and unresolved features will be presented, and prospects for applying the methods will be discussed.

1. Introduction

Over the last four decades the use of numerical flow models in oceanography has vastly increased. Models are run operationally for regional locations, ocean basins, and the entire earth. In addition, specialized research models targeting specific processes and areas are routinely produced. These models are often coupled with biological and chemical models for research into biological-physical and biogeochemical-physical interactions. The role of some models is to create conditions close to reality, in a deterministic sense, whereas others have the role of imitating mean behavior or fluctuation behavior. The role of yet another family of models is to alter conditions from reality to study the ramifications, examples being interdisciplinary climate models [1-3]. All of these models provide full access to time-evolving three-dimensional fields (4-D fields) for process studies, or for predictive purposes.

There is strong motivation for using these models for ocean acoustic studies. Suitably formulated models can include the important flow and water-mass features of the ocean, with the important features covering a wide dynamic range. Each feature has its own acoustic propagation or scattering signature, with some signatures having an interfering effect on underwater acoustic activities. The signature can be in the temporal domain, the spatial domain, or both. An important part of ocean acoustics research at this time is identifying which processes are dominant at specific times and places, and models are well suited to this.

Significant acoustic effects of water-column and seafloor features occur in concert. However, they have traditionally been studied individually, sometimes in idealized or very simple form. Despite the isolation of the processes, many of these studies have been very successful. Examples are the analysis of the Pekeris waveguide [4], adiabatic mode propagation in a smoothly varying waveguide [5], and propagation through idealized internal waves [6-8]. The state of our knowledge now demands that the full complexity be analyzed, as can be done using the ocean models. Initial efforts that have coupled four-dimensional ocean fields with 2D acoustics modeling include data assimilation and uncertainty studies [9, 10], end-to-end computations [11], real-time at-sea predictions [12] and coupled adaptive sampling [13]. In the present work, a specific focus is on 3D acoustic effects coupled to 4D ocean predictions.

We have thus motivated the use of oceanographic flow models as a straightforward approach for objective and comprehensive study of sound propagation in realistic environments, which we refer to as coupled ocean/acoustics modeling. The alternative of investigating the overall effects of simultaneously occurring feature types by constructing idealized process models with multiple features (straight line internal waves in two-layer fluid over a uniformly sloped bottom and one eddy, for example) is likely to lack objectivity or completeness. In fact, such feature models are mainly utilized to initialize ocean models or describe/assimilate specific features [14]. Coupled ocean/acoustics modeling can have high value, under the condition that the synthesized environments are sufficiently inclusive, representative, and accurate. This is a nontrivial condition; many challenges remain for flow models in terms of boundary conditions and data assimilation, resolution of near-boundary effects and mixing effects, and three-dimensional nonlinear gravity waves with hydrostatic pressure. Note that making acoustic propagation predictions, without analysis of the behavior or the mechanisms at work, is a byproduct of coupled ocean-acoustic modeling.

Coupled ocean/acoustics modeling is becoming more common. Nevertheless, the approach is relatively recent and the best research path to take at this time deserves discussion. In this paper we discuss the potential of this method, and inform the discussion with some example computations from recent work in the Mid Atlantic Bight.

2. Coupled ocean/acoustics model types and research questions

A full review of global and regional ocean flow models is beyond the scope of this paper. Suffice it to say that high-resolution state-of-the-art primitive equation ocean models are used. The state-of-the-art is for models to be forced with the best available surface and boundary fluxes, and driven towards consistency with available oceanographic data [9,10].

Although resolution of the order of one wavelength is often required for computational acoustic modeling, it is fortunate that the 3D environment being acoustically modeled is not required to have this resolution. For ocean sound propagation at low to medium frequencies (50-3500 Hz), the scale L of heterogeneity in the medium responsible for sound-field structure from propagation effects (forward scattering) is often large compared to the wavelength λ. This important scale L is at or near the Fresnel scale $R_f = (\lambda R)^{1/2}$ where R is the source-receiver separation. Because of this scale separation, environmental models may exclude medium structures at the smallest scales. This is not a rigorous rule. In addition to scattering effects, larger-scale regional or azimuthal variability of waveguide conditions can strongly influence propagation behavior.

Acoustic codes of many types are available for generating simulated sound fields within ocean-model generated environmental conditions. 2D parabolic equation codes are typically applied, often in so-called N×2D mode, giving independent in-plane simulations directed radially from a source [15]. Ray-based codes have also been used [12]. Recently we began modeling fully 3D parabolic equation simulations in data-driven model-generated environments [16]. This paper describes further results from that study. This study is of sound propagating down a canyon of order tens of kilometers. The results show strong horizontal focusing of sound, verifying that N×2D modeling is inadequate for this situation. Here are a few research questions accessible with coupled ocean/acoustic modeling:

1. When is N×2D modeling adequate? Can this be determined with bathymetric or ocean-condition metrics?
2. What are the relative predictabilities of the various ocean features?
3. How does ocean predictability map into acoustic predictability?
4. Where does one "draw the line(s)" between deterministic and statistical modeling?
5. Are biases introduced when small-scale ocean features are not resolved?

3. Models now in use

We have a few models in place for this research. One acoustic model and four ocean models are described here. 4-D acoustic modeling outputs are shown for one ocean model, illustrating the variability. Modeling shown here is for the Hudson Canyon region east of the continental United States [16]. The acoustic model and the flow model (the "Hudson Canyon Model") are described. The other flow models described here are for an area west of the continental United Stated, and from the Taiwan area.

3a. Acoustic propagation model

The model solves the parabolic wave equation on a three-dimensional Cartesian coordinate grid. The code uses the Thomson-Chapman wide-angle propagator version of the Fourier split-step marching algorithm [17]. The alteration from standard 2-D to 3-D modeling is made by replacing the one-dimensional Fourier transform pair (z, k_z) used for each marching-direction (x-direction) range step (of length Δx) with two-dimensional Fourier

transform pairs (z, y ; k_z , k_y). The model has been verified with a few benchmark tests and convergence tests. The frequency of 75 Hz is used here (wavelength λ=20 m). The grid increments are $\Delta x=\lambda$, $\Delta y=\lambda/5$, and $\Delta z=\lambda/10$ (20, 4, and 2 m, respectively). There are 2^{12} and 2^{11} grid points in the y and z directions, respectively. There is an image ocean to satisfy a flat ocean surface boundary condition, so final output is produced at only 2^{10} depths. Sound is absorbed at the domain edges with a multiplicative attenuation mask. A report summarizes the fundamentals of an earlier form of the model [18]. An important question is how to interpolate the coarse ocean model fields (o(100-m) horizontal spacing, o(50) vertical layers) to the tight acoustic grid (meters in the horizontal, hundreds of vertical layers). Such interpolation (e.g. [15]) should be ocean model dependent since it should be conservative and preserve bathymetry, volume and gradient field properties. Various schemes are being tested.

3b. Hudson Canyon Model

The Hudson Canyon Model (HCM) was constructed specifically for the Hudson Shelf Valley and Canyon area. It is based on the Regional Ocean Modeling System (ROMS; http://myroms.org) [19-21]. ROMS is a primitive-equation ocean model that uses terrain-following coordinates. It employs the hydrostatic pressure approximation. It uses a high-order time-stepping scheme, consistent temporal averaging, and accurate separation of barotropic and baroclinic modes. Modification of the barotropic pressure gradient terms to account for local variations in density, in conjunction with high-order discretization in the vertical, has greatly reduced pressure-gradient truncation errors that have hampered terrain-following coordinate models in regions of steep bathymetry, such as underwater canyons [22]. Because of the hydrostatic approximation ROMS does not accurately model internal waves steepening into bores, or short-wavelength high-frequency nonlinear internal waves. However, it does accurately model weakly nonlinear internal waves with hydrostatic pressure anomalies, although must be taken when examining features of this type.

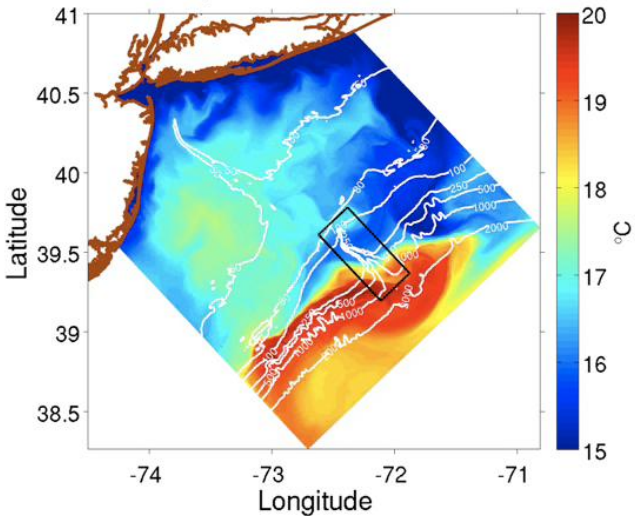

Fig. 1. A snapshot of surface temperature from the Hudson Canyon Model is shown. The time is 0000 October 27, 2009. The box indicates the boundaries for the upper panel of Fig. 2.

The HCM covers the entire Hudson Canyon and the neighboring shelf and slope seas (about 200 by 200 km). To resolve the narrow canyon (~10 km), along-shelf resolution of the model increases from 1.5 km at both ends to about 350 m around the canyon. HCM has a

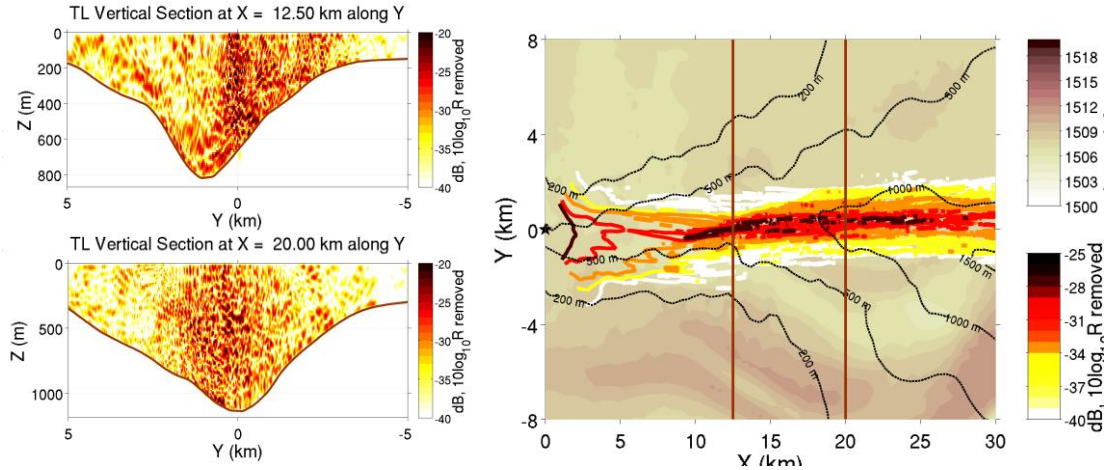

Fig. 2. At the left, two acoustic fields vertical sections calculated with the 3D PE model are shown. The sections are from one snapshot, 50-m source depth, 75 Hz. The positions of the sections are shown at the right with lines at x=12.5 km and x= 20 km from the source (star) at x=0, y=0. The right panel also shows the horizontal extent of the acoustic modeling domain. The depth-averaged sound intensity in the water contoured in color at the right. The grayscale shows the sound speed at 50-m depth in the HCM-computed environment at this snapshot (0000Z 31/Oct/2009).

cross-shelf resolution about 400 m over the entire domain, and 40 vertical layers, with dense layering near both the surface and the bottom. Forcing is a critical concern in models designed to accurately model ocean conditions. At the surface the model applies fluxes using bulk formulas, computed sea surface temperature and currents, and standard meteorological products. Data products are marine boundary layer winds, temperature, humidity, and pressure from the US National Weather Service National Centers for Environmental Prediction. Fluxes used are momentum, sensible heat, latent heat, and longwave radiation.

Initial and boundary conditions of the HCM model are from another ROMS-based model, a 7-km resolution data-assimilative Mid-Atlantic Bight model called ESPreSSO (http://www.myroms.org/espresso/), which is currently being run in real-time at Rutgers University. The Hudson River discharge data were obtained from USGS Water Data and modified to include un-gauged portions of the watershed (waterdata.usgs.gov/nwis). Tide boundary conditions are from the ADCIRC tidal database [23]. The HCM has a time increment of 15 seconds.

Fig. 1 shows a snapshot of surface temperature from the model. A very warm feature, a remnant of a warm eddy is seen, as is a cold flow feature impinging from the north. The section of Hudson Canyon that slices into the continental slope is the major bathymetric feature in the HCM sub-domain from which model fields are fed into the acoustic model, which lie in the box of Fig. 1.

3c. Southern California and Taiwan area modeling

The Southern California Bight is modeled with the MITgcm code (http://MITgcm.org). An area offshore of San Diego, CA has been modeled with 100 z levels reaching 2000 m depth, with spacing varying from 1.0 m at the surface to 30 m at depth. Horizontal grid spacing is 1003 m. Transect data are used for internal initialization Forcing is imposed at the domain boundaries, where the flow is set equal to the depth-uniform predictions of the Eastern North Pacific (ENPAC) 2003 tidal database [24]. The flow is relaxed to the ENPAC values within zones of 10 horizontal grid points to prevent the reflection of outgoing waves. Significant

internal tides are seen in the model, of the same magnitude as reported for the Hudson Canyon Model [16], 10-15 m amplitude.

Through the Quantifying, Predicting and Exploiting Uncertainty program, we have also implemented a model of the Taiwan area [9]. Briefly, this is a free-surface two-way nested primitive equation code [25]. The nesting allows high-resolution internal domains. The model was run for 2008 pilot exercise and for the intensive observation period during the fall 2009. Boundaries were forced with barotropic tidal flows computed by multi-resolution generalized inverse [26], so as to capture finer bathymetric effects. Surface forcing was from operational models. Extensive N×2D acoustic modeling has been performed with the 4D ocean fields for an area northeast of Taiwan [9]. The results show significant sound propagation time-variability from variations of larger-scale ocean transports through the Strait of Taiwan and mesoscale features, but also through the evolution of phase-resolved internal tides. The area includes many canyons, and 3D acoustic modeling is required to extend the research into the canyon areas.

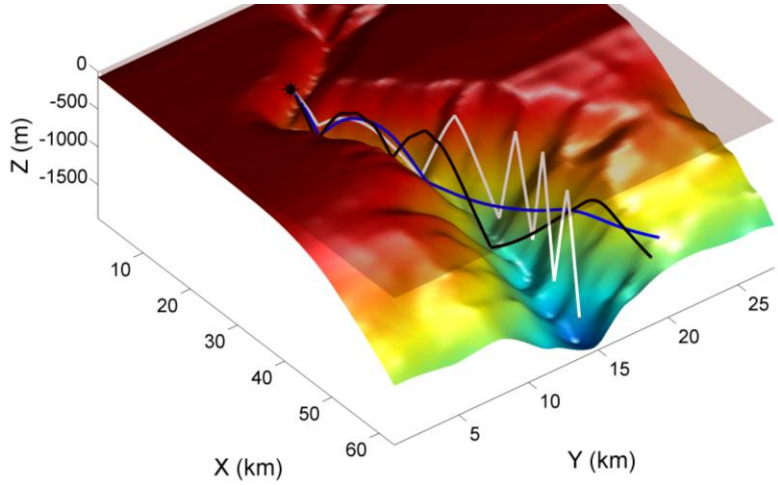

Fig. 3. Three-dimensional ray tracing using high-resolution bathymetry and the HCM output fields.

4. Hudson Canyon acoustic results

The 3D acoustic model has been run for 84 snapshots of HCM output, with a 6-hour time increment. Fig. 2 shows acoustic conditions at one time snapshot. There is significant focusing of sound in the V-shaped canyon, determined reliably by looking at depth-averaged sound, which averages over small-scale interference patterns. Reduced seafloor attenuation is a possible explanation for the higher intensity in the canyon, but comparison of N×2D and 3D fields verifies horizontal effects, as do 3D ray traces. We wish to determine the robustness in time of this effect, and, if variable, what oceanographic features drive the variability. Fig 3. shows 3-D horizontally deflected 3D rays. Fig. 4 shows, at the center, many time series of intensity along a line at 128 m depth, x = 12 km. The range from the source varies with y in these panels, and the intensity is corrected for cylindrical (max. correction 0.8 dB). The mean intensity as a function of y is plotted at the top, showing the mean focus effect at this depth. There is a very narrow focus near zero, a plateau of 10 dB below the peak that is a roughly 3 km wide, and a sharp drop off at y = -3.4 km. There is an asymmetry in the pattern associated with the lack of symmetry in the canyon. The scintillation index (SI) as a function of y is also shown in Fig. 4. The SI are near one, saturated scattering (equivalent to many randomly varying ray arrivals), for many locations. However, SI are much higher than one at large negative y, suggesting strong focusing or

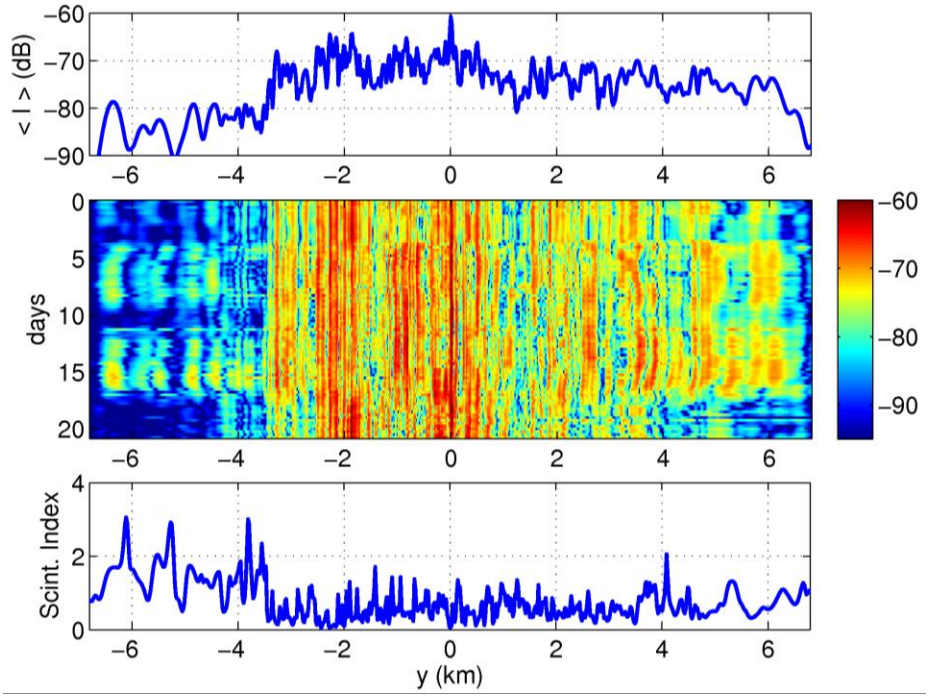

Fig. 4. Center panel: The model intensity I(y,t) at range x=12 km and depth z=128 meters depth in plotted. Upper panel: The mean over time is plotted. Lower panel: The scintillation index is plotted as a function of y. The scintillation index is the intensity variance divided by the mean intensity squared.

unusual intermittency. Fig. 5 shows an apparent relationship between mean intensity and SI, with each computed for 5760 points in the y = 12 km plane, 28 m < z < 148 m. The cause of this and the implications are not yet known.

Fig 6. shows eight individual time series that show very different behavior. The time series at y = -6 km has 15-dB oscillations every few days. This behavior is only seen for a few days at y = 6 km. The fields will be examined to determine the cause of this. The sound intensity on the shelf at negative y (across the canyon from the source) is low compared to on the shelf at positive y, and it is more stable in time. There are many short periods of time with day-scale oscillations of intensity that may be associated with internal tides.

To analyze the frequency content of the intensity variability plotted in the center of Fig. 4 we use the continuous wavelet transform (CWT) [27] and the well-known Mexican hat wavelet. Figs. 7 and 8 show the transform coefficients $C(t,s)$ as a function of time and scale

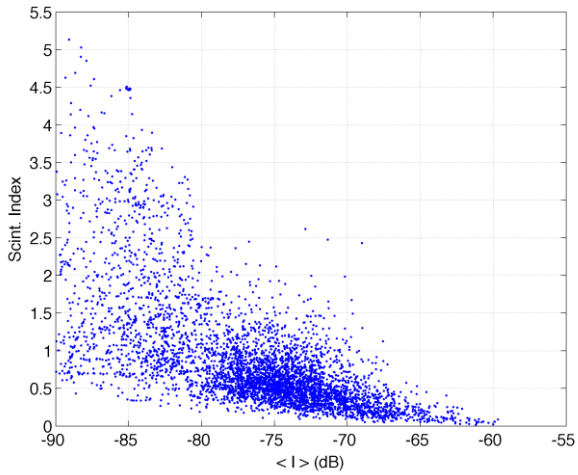

Fig. 5. Scintillation index versus mean intensity. 28 to 148 meters depth. 5760 values.

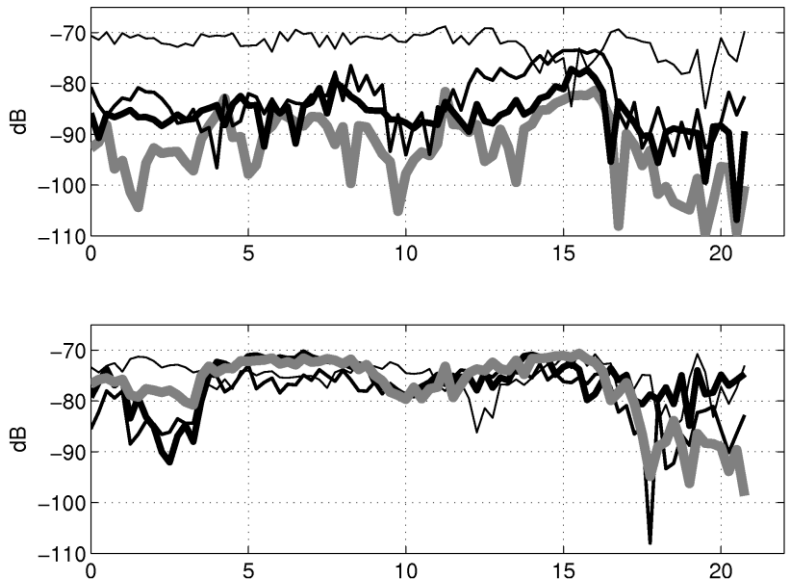

Fig. 6. Intensity at 128 m depth. Upper: Thick to thin: Intensity time series at y = -6, -5, -4 and -3 km. Lower: Thick to thin; Intensity time series at y = 6, 5, 4 and 3 km.

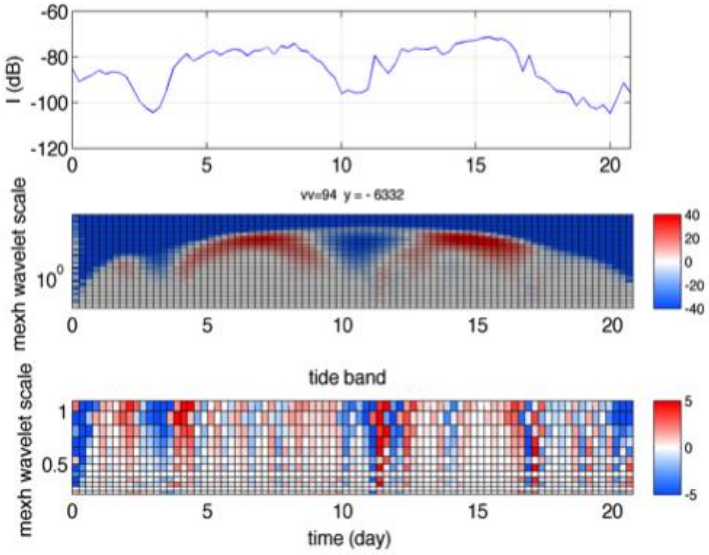

Fig. 7. Multi-scale continuous wavelet transform of intensity at 128 m depth, edge area.

factor (equivalent to frequency) for two *y* locations. Each figure shows the analyzed time series at the top, with the complete transform in the center. Fig. 7 shows the two peaks of large intensity at y of -6332. The transform maps this energy into an oscillation period of about 8 days (center panel). The lowest panel enlarges the results for the smallest wavelet elongation scale factors, which are in the tidal band. Scale factor of 1.0 corresponds to diurnal tides, 0.5 to semidiurnal tides (poorly resolved here). Weak tidal effects (a few dB) occur for many days, with peaks of activity at days 12 and 17 (the peak at day 4 is linked to the 24 dB rise in intensity). Fig. 8 shows order 10-dB tide-band oscillations days 5-8 and 10-18. There is also activity with 4-day period, 12 to 15 dB peak to peak. Use of the Morlet wavelet [27] handles the tidal signals better but the long-period signals less well.

Fig. 9 shows *y*-dependent and time-dependent CWT results $C(t,y)$ for four scaling factors. Edge effects appear as blue bands. The top panel shows intermittent activity in the semi-

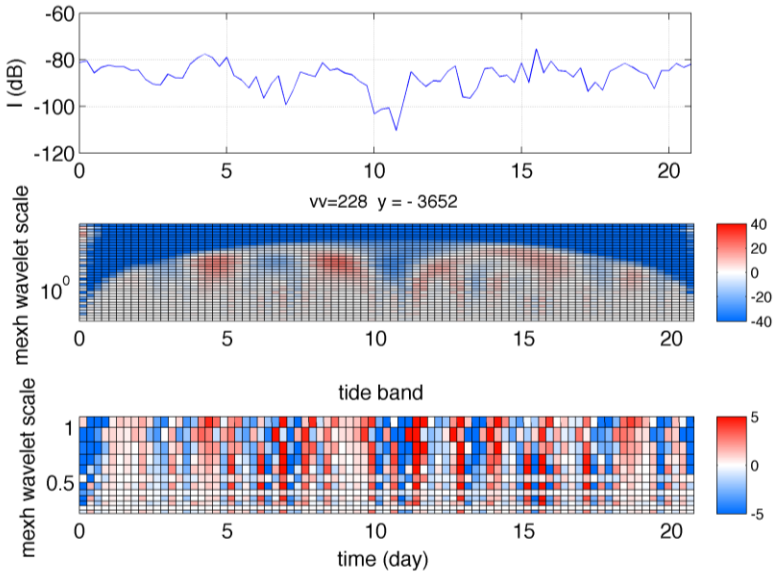

Fig. 8. Multi-scale continuous wavelet transform, y = -3652 m, of intensity at 128 m depth.

diurnal band. Below that is the diurnal band activity, which is highest at the low-*y* edge, but also apparent at many other locations. The third panel from the top shows in red the 8-day period peaks for the domain edges, which do not appear in the center of the domain above the canyon. Finally, activity at a randomly chosen 3-day period is show in the fourth panel, which has similar structure with respect to *y* as the 8-day period. Fluctuations at all frequencies are diminished in the domain center, over the canyon.

5. Summary

We have described the regional ocean models that we are now using to provide fields for studies of 3D acoustic propagation effects made with fully 3D acoustic simulations. Focusing of 75-Hz sound moving down Hudson Canyon is demonstrated. In addition to the mean focus effect, the variations of sound in and near the canyon area have received an initial examination. The areas with more intense sound have more stable sound level (low scintillation index, below one), whereas the areas of less intense sound have higher scintillation index. The high values indicate intermittency, as opposed to a Gaussian random nature. The time series of intensity show that the high scintillation index areas, which feature intensity distributions with enhanced tails, appear in the regions to either side of the canyon that have less intense sound than in the canyon. The statistical methods quantify the qualitative behavior of these regions, which is 30-dB to 40-dB variations between extremely weak sound and loud sound, possibly explainable as in-filling of shadow zones with sound as conditions change. A shift between shadow zone and arriving sound is a strong scattering effect consistent with high scintillation indices.

An initial spatially dependent time-frequency analysis of the 4D variable sound field using a wavelet transform was used in an effort to isolate the dominant phenomena causing intensity variations. This method further quantifies the differences between effects over the canyon with those beside the canyon, with effects at the majority of frequencies being stronger beside the canyon. Thus, to first order, individual point-location fluctuations at all geophysical frequencies are diminished within the canyon with respect to their levels outside the canyon. Finally, note that the tidal period acoustic fluctuations appear to be intermittent

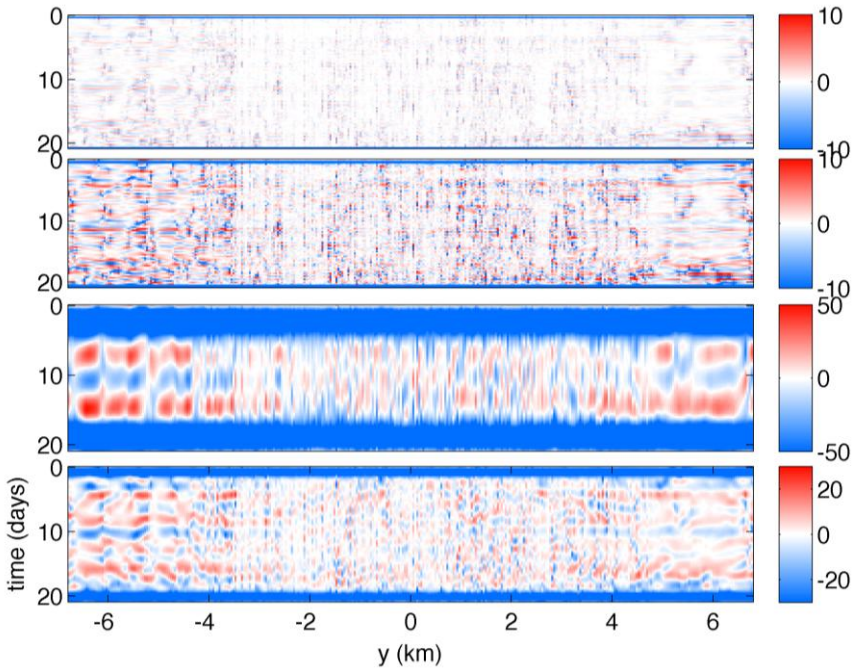

Fig. 9. Single-scale wavelet transforms in time of z =128-m intensity, at four equivalent frequencies, at all y positions. Top: semidiurnal tide frequency; next: diurnal tide; next: dominant frequency at the negative y edge of 8 days; bottom: arbitrary period, near 3 days.

over the simulation period, rather than steady state. Comparison of dynamic features and acoustic fluctuation behavior, to explain the results, remains to be done.

This analysis of 4D sound propagation in Hudson Canyon which shows that the two zones (in canyon, on shelf adjacent to canyon) have different signatures of acoustic fluctuation has not yet progresses to the point of identifying specific causes for the fluctuations. Comparison of time-dependent N×2D and 3D acoustic mode results can determine whether the time variations at specific locations are dominantly governed by 2D or 3D effects. Next, the 3D modeling can determine which areas have 3D focusing effects which are entirely determined by the seafloor geometry, and which require additional information about the water column acoustic conditions to properly compute focus patterns.

In addition to providing a method for studying the nature of 4D acoustic predictions, the linked ocean and acoustic modeling also provides a method for designing better experiments. Experiments to infer seafloor geoacoustic properties within canyons, for example, can benefit in two ways. These experiments require information about where sound interacts with the bottom, which the models can help determine. They can also determine the spectrum of natural variability that is likely to be encountered, which determines the necessary durations and sampling rates of in-situ acoustic experiments.

REFERENCES

[1] **Doney, S. C., I. Lima, J. K. Moore, K. Lindsay, M. J. Behrenfeld, T. K. Westberry, N. Mahowald, D. M. Glover, and T. Takahashi.** Skill metrics for confronting global upper ocean ecosystem-biogeochemistry models against field and remote sensing data, *J. Mar. Syst.*, **76**, pp. 95–12, 2009.

[2] **Nakicenovic, N. and R. Swart,** *Special Report on Emissions Scenarios: A Special Report of Working Group III of the Intergovernmental Panel on Climate Change*, 1st ed., Cambridge University Press, Cambridge, UK, 2000.

[3] **Thornton, P. E., S. C. Doney, K. Lindsay, J. K. Moore, N. Mahowald, J. T. Randerson, I. Fung, J.-F. Lamarque, J. J. Feddema, and Y.-H. Lee,** Carbon-nitrogen interactions regulate climate-carbon cycle feedbacks: results from an atmosphere-ocean general circulation model, *Biogeosciences*, **6**, pp. 2099–2120, 2009.

[4] **Frisk, G. V.,** *Ocean and Seabed Acoustics: A Theory of Wave Propagation*, Prentice–Hall, Englewood Cliffs, NJ, 1994. Chapter 5.

[5] **Katsnelson, B. G, V. Grigorev, M. Badiey, and J. F. Lynch**, Temporal sound field fluctuations in the presence of internal solitary waves in shallow water, *J. Acoust. Soc. Am.*, **126**, pp. EL41-EL48. 2009.

[6] **Preisig, J. C., and T. F. Duda**, Coupled acoustic mode propagation through continental shelf internal solitary waves, *IEEE J. Oceanic Eng.*, **22**, pp. 256-269, 1997.

[7] **Lin, Y.-T., T. F. Duda, and J. F. Lynch**, Acoustic mode radiation from the termination of a truncated nonlinear internal gravity wave duct in a shallow ocean area, *J. Acoust. Soc. Am.*, **126**, pp. 1752-1765, 2009.

[8] **Lynch, J. F., Y.-T. Lin, T. F. Duda and A. E. Newhall**, Acoustic ducting, reflection, refraction, and dispersion by curved nonlinear internal waves in shallow water, *IEEE J. Oceanic Eng.*, **35**, pp. 12-27, 2010.

[9] **Lermusiaux, P. F. J. and C.-S. Chiu,** Four-dimensional data assimilation for coupled physical-acoustical fields. *In Acoustic Variability, 2002*, N. G. Pace and F. B. Jensen (Eds.), Kluwer Academic Press, pp. 417-424, 2002. doi: 10.1109/JOE.2010.2068611

[10] **Lermusiaux, P. F. J., C.-S. Chiu and A. R. Robinson**, Modeling uncertainties in the prediction of the acoustic wavefield in a shelfbreak environment. *In Theoretical and Computational Acoustics 2001, Proceedings of the 5th ICTCA*, E.-C. Shang, Q. Li and T.F. Gao (Eds.), World Scientific Publishing Co., pp. 191-200, 2002.

[11] **Robinson, A. R. and P. F .J. Lermusiaux,** Systems with data assimilation for coupled ocean science and ocean acoustics, Keynote manuscript. *In Proceedings of the Sixth International Conference on Theoretical and Computational Acoustics*, A. Tolstoy, et al. (Eds), World Scientific Publishing, pp. 325-342, 2004.

[12] **Lam, F.-P. A., P. J. Haley, Jr., J. Janmaat, P. F. J. Lermusiaux, W. G. Leslie, M. W. Schouten, L. A. te Raa, and M. Rixen,** At-sea Real-time Coupled Four-dimensional Oceanographic and Acoustic Forecasts during Battlespace Preparation 2007, *J. Marine Systems*, **78**, pp. S306-S320, 2009. doi: 10.1016/j.jmarsys.2009.01.029

[13] **Xu, J., P. F. J. Lermusiaux , P. J. Haley Jr. , W. G. Leslie and O. G. Logutov,** Spatial and temporal variations in acoustic propagation during the PLUSNet07 exercise in Dabob Bay. *Proceedings of Meetings on Acoustics (POMA)*, **4**, doi: 10.1121/1.2988093, 2008.

[14] **Gangopadhyay, A., P. F. J. Lermusiaux, L. Rosenfeld, A. R. Robinson, L. Calado, H. S. Kim, W. G. Leslie and P. J. Haley, Jr.,** The California Current system: A multiscale overview and the development of a Feature-Oriented Regional Modeling System (FORMS). *Dyn. Atmos. Oceans*, in press, 2011.

[15] **Lermusiaux, P. F. J., J. Xu, C.-F. Chen, S. Jan, L. Y. Chiu and Y.-J. Yang,** Coupled ocean-acoustic prediction of transmission loss in a continental shelfbreak region: Predictive skill, uncertainty quantification and dynamical sensitivities. *IEEE J. Oceanic Eng.*, **35**, pp. 895-916, 2010.

[16] **Duda, T. F., Y.-T. Lin, A. E. Newhall, W. Zhang and J. F. Lynch**, Computational studies of time-varying three-dimensional acoustic propagation in canyon and slope regions, *In Oceans 2010 Seattle Conference Proceedings*, IEEE/MTS, 2010.

[17] **Thomson, D. J. and N. R. Chapman,** A wide-angle split-step algorithm for the parabolic equation, *J. Acoust. Soc. Am.*, **74**, pp. 1848-1854, 1983.

[18] **Duda, T. F.,** Initial results from a Cartesian three-dimensional parabolic equation acoustical propagation code, Tech. Rept. WHOI-2006-14, Woods Hole, MA, 2006.

[19] **Shchepetkin, A. F. and J. C. McWilliams,** A method for computing horizontal pressure-gradient force in an oceanic model with a nonaligned vertical coordinate, *J. Geophys. Res.*, **108**, p. 3090, doi:10.1029/2001JC001047, 2003.

[20] **Shchepetkin, A. F. and J. C. McWilliams,** The regional oceanic modeling system (ROMS): a split-explicit, free-surface, topography following coordinate oceanic model, *Ocean Modelling*, **9**, pp. 347-404, 2005.

[21] **Haidvogel, D. B., H. G. Arango, K. Hedstrom, A. Beckmann, P. Malanotte-Rizzoli, and A. F. Shchepetkin,** Model evaluation experiments in the North Atlantic Basin: Simulations in nonlinear terrain-following coordinates, *Dyn. Atmos. Oceans,* **32**, pp. 239-281, 2000.

[22] **Allen, S. E., M. S. Dinniman, J. M. Klinck, D. D. Gorby, A. J. Hewett, and B. M. Hickey,** On vertical advection truncation errors in terrain-following numerical models: Comparison to a laboratory model for up-welling over submarine canyons, *J. Geophys. Res.*, **108**, p. 3003, 2003.

[23] ADCIRC tidal databases, http://www.unc.edu/ims/ccats/tides/tides.html.

[24] **Spargo, E. A., J. J. Westerink, R. A. Luettich, Jr., and D. J. Mark,** ENPAC 2003: A tidal constituent database for Eastern North Pacific Ocean, US Army Corps of Engineers Report ERDC/CHL TR-04-12, 2004.

[25] **Haley, P.J., Jr. and P.F.J. Lermusiaux,** Multiscale two-way embedding schemes for free-surface primitive-equations in the Multidisciplinary Simulation, Estimation and Assimilation System. *Ocean Dynamics*, **60**, pp. 1497-1537, doi:10.1007/s10236-010-0349-4, 2010

[26] **Logutov, O. G. and P. F. J. Lermusiaux**. Inverse barotropic tidal estimation for regional ocean applications. *Ocean Modelling*, **25**, pp. 17-34, 2008.

[27] **Emery, W. J, and R. E Thomson**, *Data Analysis Methods in Physical Oceanography*, 2nd edition, Elsevier, Amsterdam, 2001, Chapter 5.